Tech Science Press

New Correlations for Determination of Optimum Slope Angle of Solar Collectors

Ali Khosravi[1,*], Oscar Ricardo Sandoval Rodriguez[2], Behnam Talebjedi[1], Timo Laukkanen[1], Juan Jose Garcia Pabon[3] and Mamdouh El Haj Assad[4]

[1]Department of Mechanical Engineering, School of Engineering, Aalto University, Espoo, Finland
[2]Graduate Program in Mechanical Engineering Federal University of Minas Gerais, Belo Horizonte, Brazil
[3]Institute of Mechanical Engineering, Federal University of Itajubá, Itajubá, Brazil
[4]Sustainable and Renewable Energy Engineering Department, University of Sharjah, Sharjah, United Arab Emirates
*Corresponding Author: Ali Khosravi. Email: Ali.khosravi@aalto.fi
Received: 14 April 2020; Accepted: 06 July 2020

Abstract: The energy coming from solar radiation could be harvested and transformed into electricity through the use of solar-thermal power generation and photovoltaic (PV) power generation. Placement of solar collectors (thermal and photovoltaic) affects the amount of incoming radiation and the absorption rate. In this research, new correlations for finding the monthly optimum slope angle (OSA) on flat-plate collectors are proposed. Twelve equations are developed to calculate the monthly OSA by the linear regression model, for the northern and the southern hemisphere stations from 15° to 55° and –20° to –45°, respectively. Also, a new equation for calculating the yearly tilt angle is developed and compared with several other calculation methods from the literature. Results confirm a 20% increase in solar energy absorption by adjusting the collectors' tilt angle in monthly time periods. This is while the adjusted collectors with the yearly optimum slope angle receive approximately 7% higher solar radiation compared to the horizontal collectors. Furthermore, the proposed equations outperformed the other calculation methods in the literature.

Keywords: Photovoltaic system; flat-plate collector; slope angle; solar energy; optimum slope angle; linear regression

Nomenclature

$\bar{H}$:	monthly average solar radiation (MJ/m^2)
$\bar{H}_d$:	monthly average daily defuse radiation (MJ/m^2)
$\bar{K}_T$:	monthly average clearness index
OSA:	optimum slope angle
PV:	photovoltaic
RMSE:	root mean square error

Greek Symbols

ρ_g:	ground reflectance factor
β:	slope angle (°)
δ:	declination angle
γ:	azimuth angle (°)

φ: latitude (°)
ω_s':   sunset hour angle

Subscripts/Superscripts
T: total
b: beam radiation
d: diffuse radiation
R: reflected radiation
opt: optimum

1 Introduction

Energy demand is increasing rapidly across the world, because of population and economic growth, more specifically for electricity, heat and transportation [1]. On the other hand, utilizing fossil fuels for energy generation leads to an increase in greenhouse gas emissions resulting in global warming [2]. Therefore, utilizing clean energy sources for energy generation is becoming crucially important [3,4]. This issue can bring up a lot of challenges and opportunities. A sustainable and renewable future requires new attitudes and new systems, which are technically efficient and economically viable. If we want to combat global warming and save the planet, we should develop modern energy systems, improve the conventional energy systems and use energy more efficiently. Renewable energy sources that mostly referred to as clean energy, originate from natural sources or those processes that are constantly replenished. In recent years, replacing fossil fuel energy systems by renewable energy systems have been received a lot of attentions [5,6].

Solar energy is the most popular method of energy production worldwide, due to its wide availability and low cost of use anywhere in the world [7–9]. Using science and technology is important for improving the exploitation of this sort of energy production systems. Solar cells (also called photovoltaic (PV) cells by scientists) directly convert sunlight energy into electricity. Flat plate collectors (solar thermal collectors and photovoltaic systems) are very popular for collecting solar energy, and many optimizations have been conducted to increase the collectors' efficiency [10–12]. Optimizing the collector slope angle (SA) could be one of the main actions to improve the energy efficiency of the solar panels.

Some scholars developed expressions to find the yearly optimum slope angle (OSA) [13–20]. Talebizadeh et al. [21] proposed 12 equations for the OSA of six cities in Iran. On the other research, Talebizadeh et al. [22] utilized a genetic algorithm to predict the optimum slope and azimuth angles. They showed the high dependency of the beam solar radiation on the optimum slope angle. Also, Nijegorodov et al. [23] developed one equation for each month of the year to estimate the optimum slope angle. Elminir et al. [24] proposed a mathematical model for determining the slope angle in order to find the maximum solar radiation on the flat-plate collectors for Helwan city in Egypt. Also, Kacira et al. [25] developed a similar method to find the optimum tilt angle and orientations of photovoltaic panels in Sanliurfa, Turkey. They determined the monthly tilt angle with the minimum value as 13° in June and the maximum value as 61° in December. Benghanem et al. [17] investigated the maximum accessible absorbed solar radiation on flat-plate collectors by optimizing the tilt angle for Madinah in Saudi Arabia. Based on their research, the optimum annual tilt angle should be roughly equal to the location latitude. Jamil et al. [19] performed a comprehensive investigation of the optimum tilt angle in ten different stations in the world. Jamil et al. investigated the slope angle selection for flat-plate collectors in a theoretical way. Ulgen [26] determined the OSA for solar collectors in Izmir (Turkey). Ulgen estimated the total solar radiation on a tilted surface by mathematical model and finally calculated the optimum tilt angle for this area. Slope angles were determined by different values between 0° in June to 61° in December for Izmir, Turkey.

For the maximum solar radiation, the collector's surface should be adjusted in a way to be perpendicular to the sun's rays. Solar trackers are able to adjust the collector's surface to follow the sun instantaneously. But these kinds of trackers are capital intensive. The other option is to change the collector's surface angle manually. In this study, a comprehensive research on tilt angle solar collectors with several stations in northern and southern hemispheres is performed. A new correlation for calculating the yearly tilt angle is proposed. Also, 12 equations for determining the monthly optimum tilt angle using the linear regression model are proposed, which are compared to the other equations in the literature. All developed correlations are tested with new stations in northern and southern hemispheres.

2 Material and Methods

In this section, the mathematical modeling of this study has been provided. We explain two different methods (Liu et al. [27] and Klein et al. [28]) to compute the monthly average of daily radiation on the solar collectors.

2.1 Liu and Jordan Method

Eq. (1) provides the monthly average of daily radiation on the tilted surface by considering the contributions of the beam radiation, diffuse radiation, and the reflected radiation from the ground. This method was developed by Liu et al. [27] and extended by Klein [29]. In this method, collectors are considered with azimuth angle (γ) of $0°$ and $180°$ for northern and southern hemispheres, respectively [15]. According to Duffie et al. [30], the total monthly average daily radiation is defined as:

$$\bar{H}_T = \bar{H}_b \bar{R}_b + \bar{H}_d \left(\frac{1 + \cos \beta}{2}\right) + \rho_g \bar{H} \left(\frac{1 - \cos \beta}{2}\right) \tag{1}$$

In another form, we have:

$$\bar{R} = \frac{\bar{H}_T}{\bar{H}} = \left(1 - \frac{\bar{H}_d}{\bar{H}}\right) \bar{R}_b + \frac{\bar{H}_d}{\bar{H}} \left(\frac{1 + \cos \beta}{2}\right) + \rho_g \left(\frac{1 - \cos \beta}{2}\right) \tag{2}$$

where $\bar{H}_d/\bar{H}$ is a function of $\bar{K}_T$, and could be obtained by the following equations:

$$\frac{\bar{H}_d}{\bar{H}} = 1.391 - 3.560 \, \bar{K}_T + 4.189 \, \bar{K}_T^2 - 2.137 \, \bar{K}_T^3 \; (\omega_s \leq 81.4°, \; 0.3 \leq \bar{K}_T \leq 0.8) \tag{3}$$

$$\frac{\bar{H}_d}{\bar{H}} = 1.311 - 3.022 \, \bar{K}_T + 3.427 \, \bar{K}_T^2 - 1.821 \, \bar{K}_T^3 \; (\omega_s > 81.4°, \; 0.3 \leq \bar{K}_T \leq 0.8) \tag{4}$$

Also, $\bar{R}_b$ is the average daily beam radiation rate on the tilted surface for the month that is equal to $\bar{H}_{bT}/\bar{H}_b$. For the surfaces that are sloped toward the equator in the northern hemisphere with $\gamma = 0°$:

$$\bar{R}_b = \frac{\cos(\varphi - \beta) \, \cos \delta \, \sin \omega_s' + (\pi/180)\omega_s' \, \sin(\varphi - \beta) \, \sin \delta}{\cos \varphi \, \cos \delta \sin \omega_s + (\pi/180)\omega_s \, \sin \varphi \, \sin \delta} \tag{5}$$

In which, φ, β, and δ are latitude, slope angle, and declination angle. δ is the angular position of the sun at solar noon with respect to the plane of the equator, which is presented in Eq. (6).

$$\delta = 23.45 \sin \left(360 \frac{284 + n}{365}\right) \tag{6}$$

Also ω_s' is given in Eq. (7) which is the sunset hour angle for the tilted surface for the mean day of the month, which is given by:

$$\omega_s' = \min \left[\begin{array}{l} \cos^{-1}(-\tan\varphi.\tan\delta) \\ \cos^{-1}(-\tan(\varphi - \beta)\,\tan\delta) \end{array} \right] \tag{7}$$

For the collectors in the southern hemisphere that are sloped toward the equator, with $\gamma = 180°$,

$$\bar{R}_b = \frac{\cos(\varphi + \beta)\ \cos\delta\ \sin\omega_s' + (\pi/180)\omega_s'\ \sin(\varphi + \beta)\ \sin\delta}{\cos\varphi\ \cos\delta\sin\omega_s + (\pi/180)\omega_s\ \sin\varphi\ \sin\delta} \tag{8}$$

And

$$\omega_s' = \min \left[\begin{array}{l} \cos^{-1}(-\tan\varphi \cdot \tan\delta) \\ \cos^{-1}(-\tan(\varphi + \beta)\,\tan\delta) \end{array} \right] \tag{9}$$

The monthly mean daily extraterrestrial radiation is defined by Eq. (10).

$$\bar{H}_o = \frac{24 \times 3600}{\pi} G_{sc} \left(1 + 0.033\cos\frac{360\,n}{365} \right) \times \left[\cos\varphi\ \cos\delta\ \sin\omega_s + \frac{\pi\omega_s}{180}\sin\varphi\ \sin\delta \right] \tag{10}$$

In which, G_{sc} is the energy from the sun per unit of time received on a unit area of the surface perpendicular to the direction of propagation of the radiation at a mean earth-sun distance outside the atmosphere which is equal to 1367 w/m^2.

2.2 Klein and Theilacker (KT) Method

An alternative method to calculate the value of solar radiation on sloped surfaces is proposed by Klein et al. [28], considering both slope and azimuth angles. The $\bar{R}$ definition in this method is given by the following equations:

$$\bar{R} = D + \frac{\bar{H}_d}{\bar{H}} \left(\frac{1 + \cos\beta}{2} \right) + \rho_g \left(\frac{1 - \cos\beta}{2} \right) \tag{11}$$

where

$$D = \left\{ \begin{array}{l} \max\,(0,\ G(\omega_{ss}, \omega_{sr}))\ \ \text{if}\ \omega_{ss} \geq \omega_{sr} \\ \max(0, [G(\omega_{ss}, -\omega_s) + G(\omega_s, \omega_{sr})])\ \ \text{if}\ \omega_{sr} > \omega_{ss} \end{array} \right. \tag{12}$$

where $G(\omega_1, \omega_2)$ can be determined by:

$$\begin{aligned} G(\omega_1, \omega_2) = \frac{1}{2d} &\left[\left(\frac{bA}{2} - \acute{a}B \right) (\omega_1 - \omega_2)\frac{\pi}{180} + \left(\acute{a}A - bB \right)(\sin\omega_1 - \sin\omega_2) - \acute{a}\,C(\cos\omega_1 - \cos\omega_2) \right. \\ &\left. + \left(\frac{bA}{2} \right)(\sin\omega_1\ \cos\omega_1 - \sin\omega_2\ \cos\omega_2) + \left(\frac{bC}{2} \right) \left(\sin^2_{w_1} - \sin^2_{w_2} \right) \right] \end{aligned} \tag{13}$$

In which, $\acute{a}$ is:

$$\acute{a} = a - \frac{\bar{H}_d}{\bar{H}} \tag{14}$$

Also, ω_{sr} and ω_{ss} are introduced by Eqs. (15) and (18).

$$|\omega_{sr}| = \min\left[\omega_s, \cos^{-1}\frac{AB + C\sqrt{A^2 - B^2 + C^2}}{A^2 + C^2}\right] \tag{15}$$

$$\omega_{sr} = \begin{cases} -|\omega_{sr}| \text{ if } (A > 0 \text{ and } B > 0) \text{ or } (A \geq B) \\ +|\omega_{sr}| \text{ otherwise} \end{cases} \tag{16}$$

$$|\omega_{ss}| = \min\left[\omega_s, \cos^{-1}\frac{AB - C\sqrt{A^2 - B^2 + C^2}}{A^2 + C^2}\right] \tag{17}$$

$$\omega_{ss} = \begin{cases} +|\omega_{ss}| \text{ if } (A > 0 \text{ and } B > 0) \text{ or } (A \geq B) \\ -|\omega_{ss}| \text{ otherwise} \end{cases} \tag{18}$$

In which, A, B, and C are:

$$A = \cos\beta + \tan\varphi \, \cos\gamma \sin\beta \tag{19}$$

$$B = \cos\omega_s \, \cos\beta + \tan\delta \, \sin\beta \, \cos\gamma \tag{20}$$

$$C = \frac{\sin\beta \, \sin\gamma}{\cos\varphi} \tag{21}$$

As well as, a, b, and d are constant-coefficients given by the following equations:

$$a = 0.4090 + 0.5016 \sin(\omega_s - 60) \tag{22}$$

$$b = 0.6609 - 0.4767 \sin(\omega_s - 60) \tag{23}$$

$$d = \sin(\omega_s) - \frac{\pi}{180}\cos(\omega_s) \tag{24}$$

Fig. 1 demonstrates the slope angle (β) and azimuth angle (γ) for a tilted surface according to coordinate axes. Collectors are assumed to be towards the south (in the northern hemisphere), and north (in the southern hemisphere).
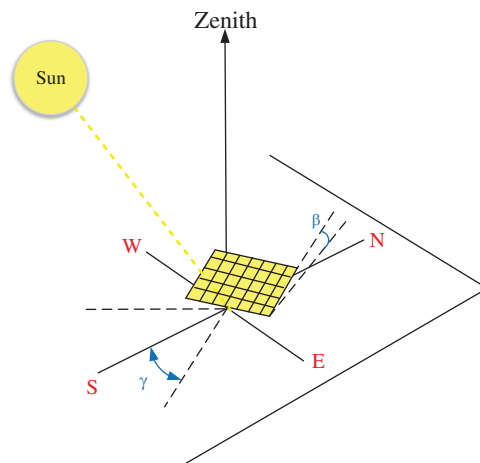
Figure 1: Surface azimuth angle and slope angle for a tilted collector
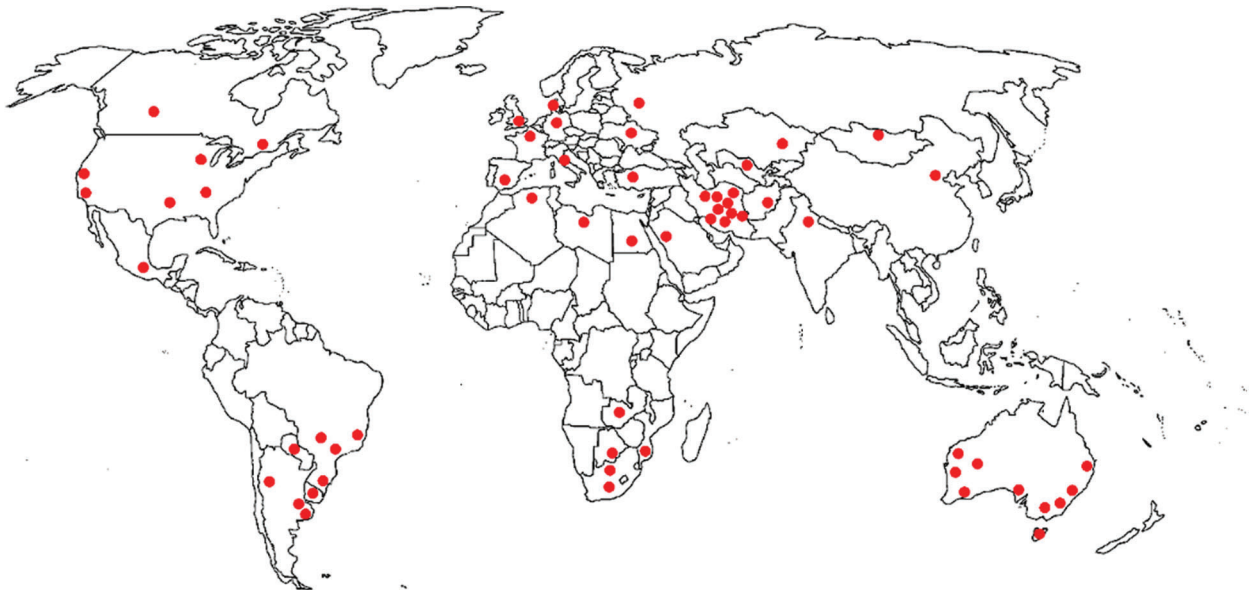
Figure 2: Selected stations on the world map

Fig. 2 shows the investigated stations in this study. The latitude in the northern hemisphere and southern hemisphere are respectively from 15 to 55° and –20 to –45°.

3 Result and Discussion

Fig. 3 illustrates the amount of average top of atmosphere insolation, average insolation incident on a horizontal surface, and average solar radiation on tilted collectors with an optimum tilt angle in Bushehr, Iran. It can be seen from the graph that the amount of the absorbed solar radiation in January, February, October, November, and December is more impressive than the other months of the year in the optimum slope angle. In January and December, the average insolation incident using the optimum tilt angle increases by approximately 50%. This is while there is no significant variation in May, June, July, and August.
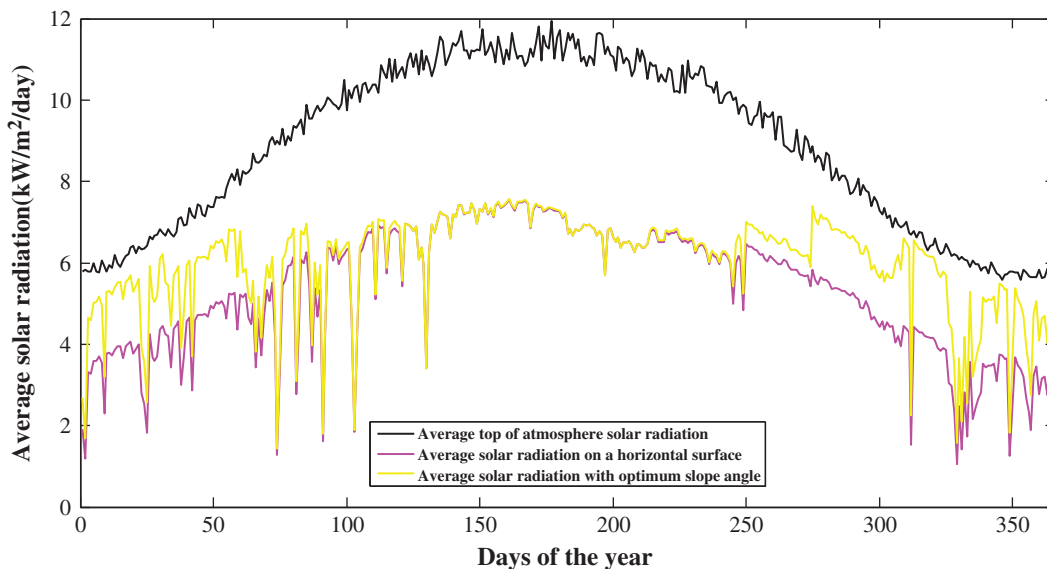
Figure 3: Daily solar radiation above the atmosphere (for a horizontal surface, and tilted collectors in Bushehr, Iran)

In this section, the value of the azimuth angle for two sample stations in the northern hemisphere (Bushehr, Iran) and southern hemisphere (Melbourne, Australia) is investigated using the KT method. The results verify that the assumption of Liu et al. [27] for $\gamma = 0°$ and $\gamma = 180°$ for the northern and southern hemisphere is acceptable. Figs. 4 and 5 express the variation of total solar radiation (MJ/m^2) on tilted collectors in all the months of the year versus the variation of azimuth angle. The optimum azimuth angle for Bushehr (Iran) in the northern hemisphere (Fig. 4) is obtained as $0°$, and for Melbourne (Australia) in the southern hemisphere (Fig. 5) as $180°$. Tab. 1 shows the selected stations in the northern hemisphere for this analysis. The latitude of places was brought in the table, and the optimum tilt angles have been calculated by Eqs. (1)–(11). Tab. 2 presents the selected stations in the southern hemisphere.
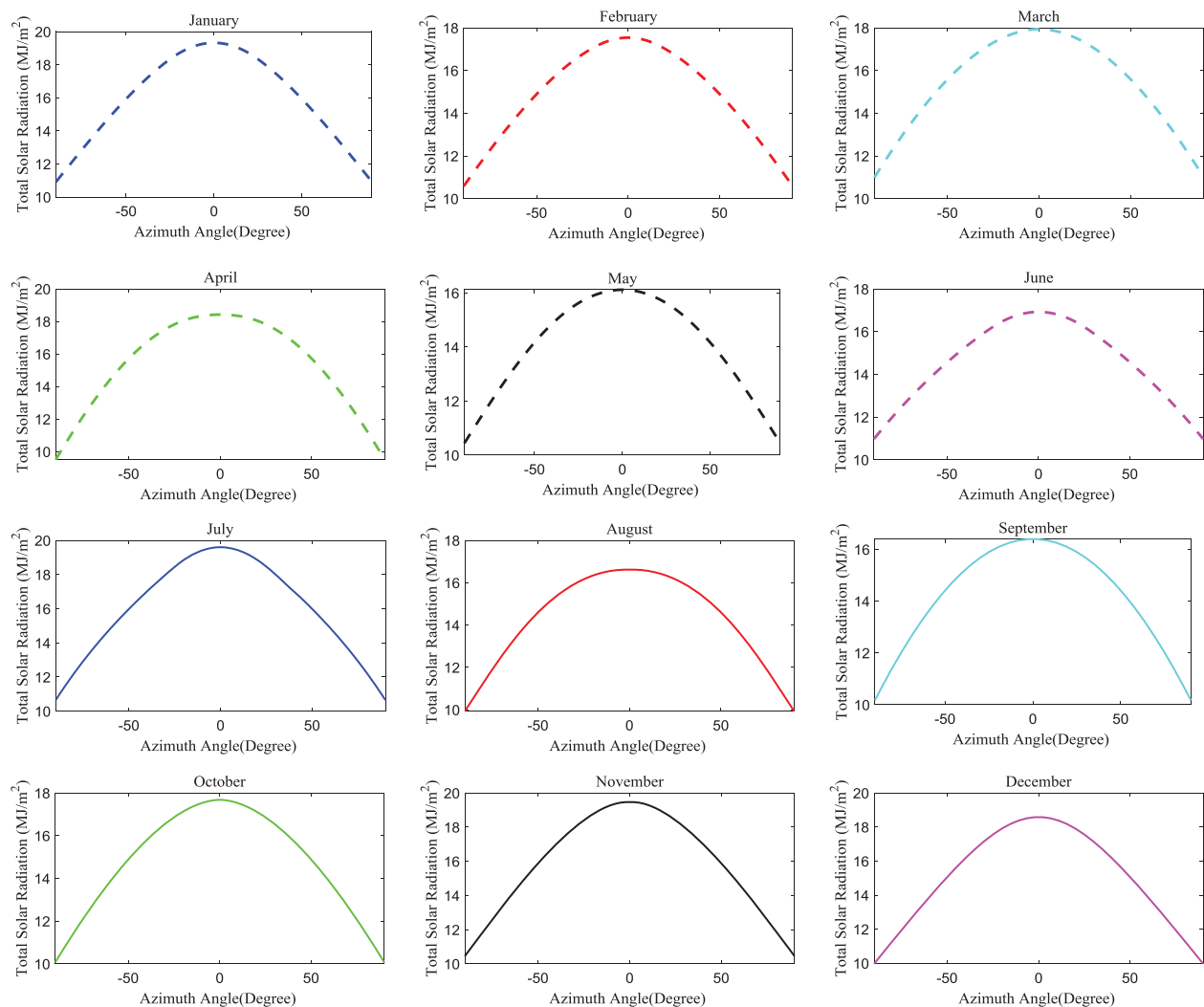
Figure 4: Optimum azimuth angle for Bushehr (Iran) in the northern hemisphere

Nijegorodov et al. [23] introduced monthly equations for the latitudes between $60°$ in the south and $60°$ in the north. Also, Talebizadeh et al. [21] developed 12 equations for a monthly optimum slope angle for latitudes of $20°$ to $40°$ in the north (Iran). In this study, in the northern (Tab. 3) and the southern hemisphere (Tab. 4), monthly equations for optimum slope angles are developed using the simple regression model. This work was undertaken by fitting a line ($y = \beta_0 + \beta_1 X + \varepsilon$), in which y is the
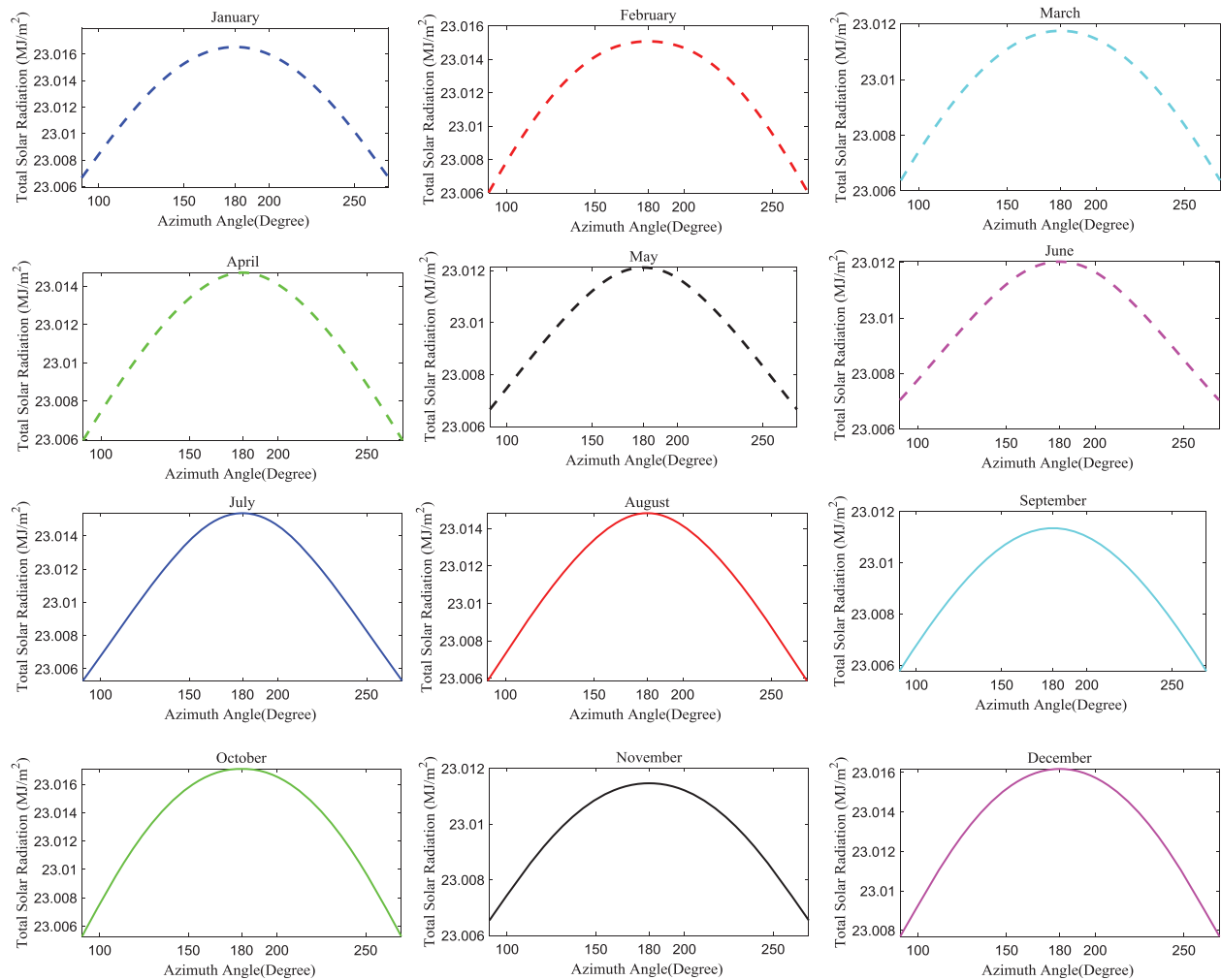
Figure 5: Optimum azimuth angle for Melbourne (Australia) in the southern hemisphere

predicted data of the dependent variable (y) for any given value of the independent variable X, β_0 is the intercept, and ε is error) to the OSA data. This line creates a relationship between two quantitative variables that are β_{opt} and $\varnothing$. Besides, for each section, one correlation for the yearly tilt angle is reported in Tabs. 3 and 4.

Fig. 6 illustrates the monthly optimum slope angle test. The graph provides a comparison between the monthly optimum tilt angle, which has been developed by Li et al. [27], Nijeogorodov et al. [23], Talebizade et al. [21] and the monthly optimum tilt angle, which is developed in this article. From the graph, root mean square error($RMSE$) value for Nijeogorodov [23], Talebizadeh [21], and this study are $2.678°$, $2.91°$, and $0.54°$, respectively. It is clear that the lowest $RMSE$ belongs to the developed correlation introduced within this study.

For the correlations test, three stations in the northern hemisphere, as well as three stations in the southern hemisphere, are considered. Ankara (Turkey), Baghdad (Iraq), and Washington (USA) in the northern and Cordova (Argentina), Porto Elizabeth (South Africa), and Esperance (Australia) in the southern for testing correlations are selected. Fig. 7 demonstrates the optimum slope angle for the six stations mentioned in the previous section. The amount of solar radiation on the slope surface is

Table 1: Selected stations in the NH with latitude and monthly OSA

	φ	Jan.	Feb.	Mar.	Apr.	May	Jun.	Jul.	Aug.	Sep.	Oct.	Nov.	Dec.
Algiers	36.8	59	51	36	18	4	–3	0	14	31	46	59	62
Arak	34.1	59	51	34	17	2	–5	–2	12	30	46	57	61
Astana	51.1	73	65	51	32	17	7	12	26	44	61	72	75
Atlanta	32.6	56	48	32	16	1	–5	–2	10	26	43	55	59
berlin	52.5	73	65	48	31	16	7	11	25	41	59	70	75
Birjand	32.9	57	48	32	16	1	–6	–3	11	29	45	56	60
Bushehr	28.9	55	46	30	13	–2	–9	–6	7	25	43	53	57
Cairo	30.1	55	45	31	14	–1	–8	–5	8	25	42	53	57
Chicago	42	65	56	40	22	8	0	4	18	34	52	62	66
Dallas	32.9	55	47	32	15	1	–6	–3	10	26	43	54	58
Edmundston	47.3	69	61	44	26	12	4	8	21	38	54	65	70
Esfahan	32.5	58	50	33	16	1	–6	–3	10	28	45	56	60
Istanbul	41	62	54	39	22	8	–1	4	18	35	51	61	63
Kabul	34.5	59	50	34	17	2	–5	–2	12	30	48	59	62
Koebenhavn	55.6	69	66	52	35	19	10	14	29	46	63	73	75
Kerman	30.3	54	45	30	13	–1	–8	–5	8	26	42	54	57
Khartoum	15.7	44	35	19	1	–13	–18	–16	–5	11	29	42	47
Kyiv	50.4	68	58	46	26	14	6	11	24	40	57	62	69
London	51.5	67	59	44	28	14	6	10	23	40	58	68	69
Los Angeles	33.9	58	50	34	17	2	–5	–2	11	28	45	57	61
Madrid	40.4	67	59	44	28	14	6	10	23	40	58	68	69
Mashhad	36.3	59	51	33	18	4	–4	0	14	32	48	59	62
Mexico City	19.4	45	37	21	4	–9	–14	–12	–2	13	30	43	49
Milan	45.4	63	56	42	25	11	2	7	20	37	53	61	65
Montreal	45.6	68	61	45	26	11	2	7	20	37	54	64	70
Moscow	55.8	75	69	54	33	19	10	14	28	44	61	70	76
New Delhi	28.6	55	46	31	13	–3	–9	–5	6	23	41	53	57
Paris	48.8	64	57	42	26	12	4	9	22	38	55	66	65
Peking	39.9	63	55	39	21	6	–1	2	14	31	49	61	65
Riyadh	24.7	49	41	25	8	–5	–11	–9	3	20	37	50	53
San Francisco	37.6	60	52	37	20	5	–3	1	15	32	49	59	63
Shiraz	29.5	55	45	31	13	–2	–9	–5	7	25	42	54	58
Tashkent	41.3	61	56	39	23	9	–1	4	19	37	53	63	65
Tehran	35.7	59	51	34	18	3	–4	–1	13	31	48	58	62
Tripoli	32.7	57	49	34	16	1	–6	–3	10	27	43	55	58
Ulan Bator	47.9	72	64	49	29	13	4	8	22	40	60	70	74
Yazd	31.9	56	47	32	14	0	–7	–4	10	28	44	55	59

Table 2: Selected stations in the SH with latitude and monthly optimum slope angle

	φ	Jan.	Feb.	Mar.	Apr.	May	Jun.	Jul.	Aug.	Sep.	Oct.	Nov.	Dec.
Adelaied	−35	1	12	28	45	57	62	61	50	34	17	2	−4
Albany	−34.9	−1	11	27	42	55	60	58	49	33	16	2	−4
Bahia Blanca	−38.7	2	15	31	50	62	64	61	50	33	18	5	−2
Buenos Aires	−34.6	−1	11	27	44	56	61	59	50	34	16	2	−5
Campinas	−23	−9	1	16	34	46	52	50	40	23	6	−7	−12
Canberra	−35.3	−1	12	29	45	57	61	60	51	35	18	3	−4
Curitiba	−25.4	−6	3	15	30	43	50	50	38	22	7	−5	−9
Johannesburg	−26.3	−7	4	20	38	52	57	55	44	28	9	−5	−10
Kimberley	−28.8	−6	7	23	41	54	59	57	47	31	12	−3	−9
Maputo	−25.9	−7	4	20	37	50	55	53	42	26	9	−5	−10
Melbourne	−37.8	1	14	30	46	58	62	60	51	35	18	4	−3
Mendoza	−32.8	−3	10	27	44	55	59	57	49	32	15	0	−6
Montevideo	−34.9	−1	11	27	44	57	61	59	50	34	16	2	−4
New Castel	−32.9	−2	9	25	42	55	60	58	49	33	15	0	−6
Porto Alegre	−30	−4	7	22	39	51	59	55	43	28	12	−2	−7
Sau Paulo	−23.6	−7	2	15	31	43	50	48	37	20	6	−6	−10
Sydney	−33.9	−2	10	26	42	55	60	58	50	34	16	1	−5
Tasmania	−41.2	4	17	32	49	61	65	63	53	37	21	7	−1
Perth	−31.9	−3	10	27	43	55	59	57	47	32	15	0	−7
Geraldton	−28.8	−6	7	24	40	52	57	55	45	30	12	−3	−9
Yalgoo	−29.3	−5	7	24	40	52	57	55	45	30	13	−2	−9
Gaborone	−24.7	−8	3	19	37	50	55	53	43	27	8	−6	−12

Table 3: Monthly and yearly OSA for the northern hemisphere

	Equations	R	R²
Jan.	$\beta_{opt} = 0.730\varnothing + 32.859$	0.961	0.923
Feb.	$\beta_{opt} = 0.796\varnothing + 22.311$	0.971	0.943
Mar.	$\beta_{opt} = 0.826\varnothing + 5.687$	0.976	0.953
Apr.	$\beta_{opt} = 0.788\varnothing - 10.274$	0.981	0.962
May	$\beta_{opt} = 0.783\varnothing - 24.556$	0.985	0.971
Jun.	$\beta_{opt} = 0.677\varnothing - 28.074$	0.983	0.966
Jul.	$\beta_{opt} = 0.746\varnothing - 27.092$	0.985	0.970
Aug.	$\beta_{opt} = 0.811\varnothing - 16.396$	0.984	0.968
Sep.	$\beta_{opt} = 0.807\varnothing$	0.973	0.947
Oct.	$\beta_{opt} = 0.816\varnothing + 17.528$	0.972	0.944
Nov.	$\beta_{opt} = 0.719\varnothing + 32.019$	0.958	0.918
Dec.	$\beta_{opt} = 0.696\varnothing + 36.550$	0.964	0.929
Yearly	$\beta_{opt} = 0.76575\varnothing + 3.38$		

Table 4: Monthly and yearly OSA for the southern hemisphere

	Equations	R	R²
Jan.	$\beta_{opt} = -0.677\varnothing - 24.119$	0.985	0.970
Feb.	$\beta_{opt} = -0.850\varnothing - 18.142$	0.994	0.989
Mar.	$\beta_{opt} = -0.937\varnothing - 5.108$	0.960	0.922
Apr.	$\beta_{opt} = -0.929\varnothing + 11.906$	0.929	0.863
May	$\beta_{opt} = -0.892\varnothing + 25.504$	0.921	0.848
Jun.	$\beta_{opt} = -0.733\varnothing + 35.434$	0.932	0.869
Jul.	$\beta_{opt} = -0.717\varnothing + 33.988$	0.945	0.894
Aug.	$\beta_{opt} = -0.811\varnothing + 21.073$	0.926	0.858
Sep.	$\beta_{opt} = -0.815\varnothing + 4.965$	0.913	0.834
Oct.	$\beta_{opt} = -0.829\varnothing - 12.591$	0.983	0.966
Nov.	$\beta_{opt} = -0.766\varnothing - 24.744$	0.997	0.993
Dec.	$\beta_{opt} = -0.609\varnothing - 25.817$	0.977	0.955
Yearly	$\beta_{opt} = -0.76575\varnothing + 3.38$		
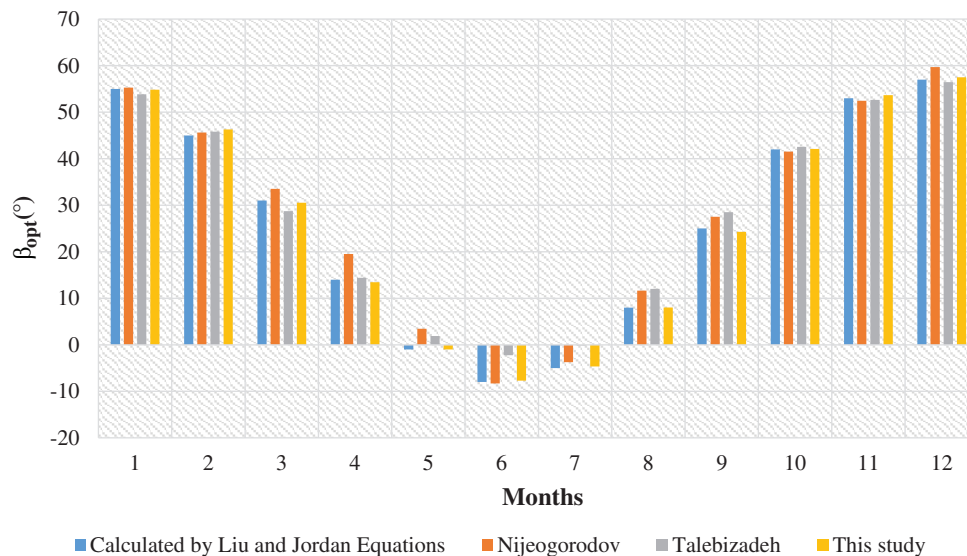
Figure 6: Comparison of the proposed correlation with that noted in the literature

calculated by different slope angles. Fig. 7 provides the optimum slope angle for these collectors on a monthly basis. Also, the values of the optimum tilt angles for each station by the proposed correlations have been shown in Fig. 8. The results show the great ability of all the proposed equations to predict the tilt angles of the solar collectors.

Average monthly radiation on flat-plate collectors is shown in Fig. 9, for Bushehr. The results show an increase in the absorbed solar energy by adjusting the collector at a monthly optimum tilt angle. This increase is approximately 20% for an annual period. Heywood et al. [13], Lunde et al. [14], and Duffie et al. [15] proposed equations to calculate the monthly tilt angle for solar collectors. Regarding the graph, by
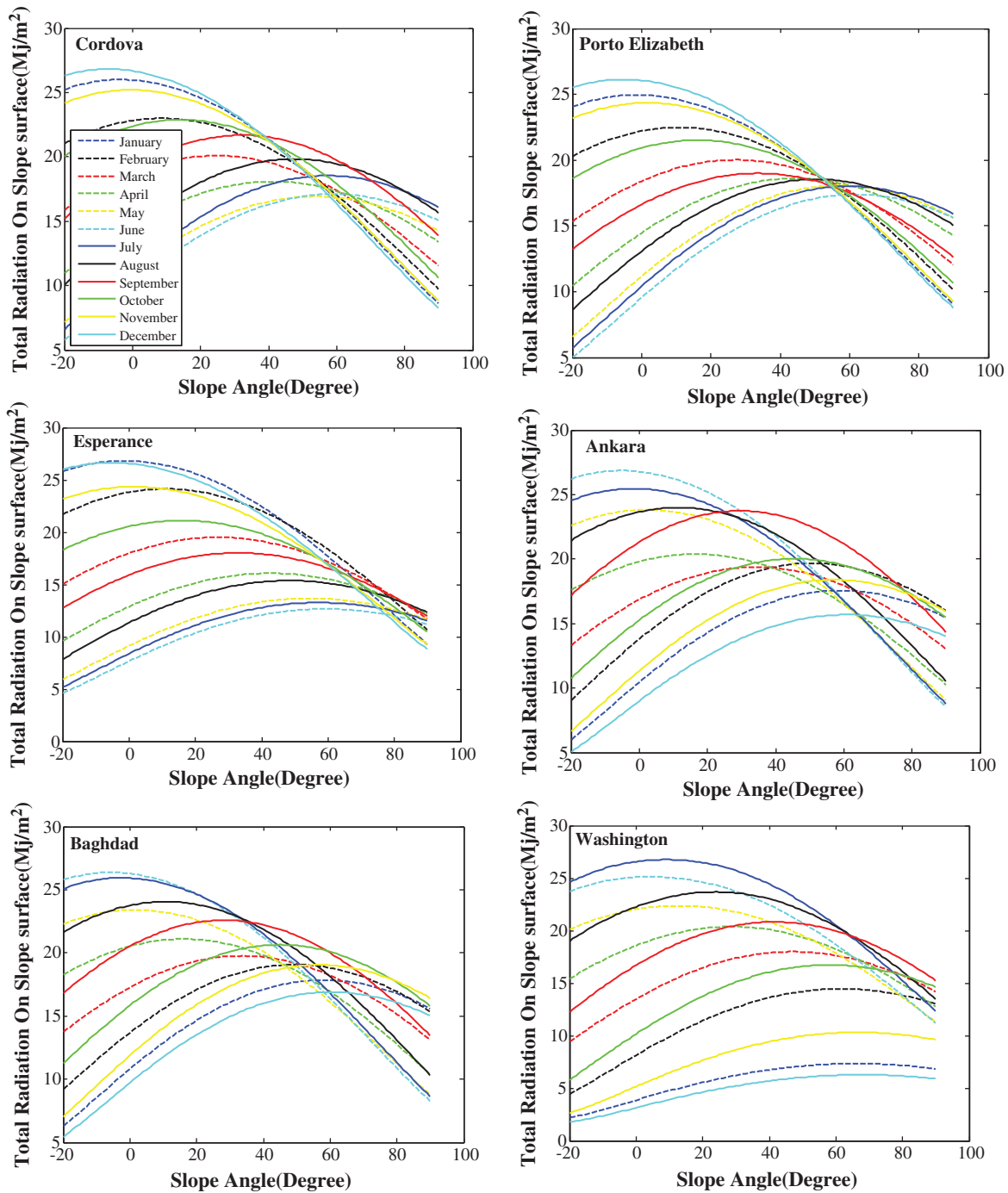
Figure 7: Evolution of total solar radiation on the slope surface as a function of the slope angle for six stations and determined by OSA

adjusting the collectors with a monthly optimum tilt angle, the value of solar radiation over the collectors is 20% more than the horizontal collectors. This increase is more than 20% in January and December and is observed close to 50%.
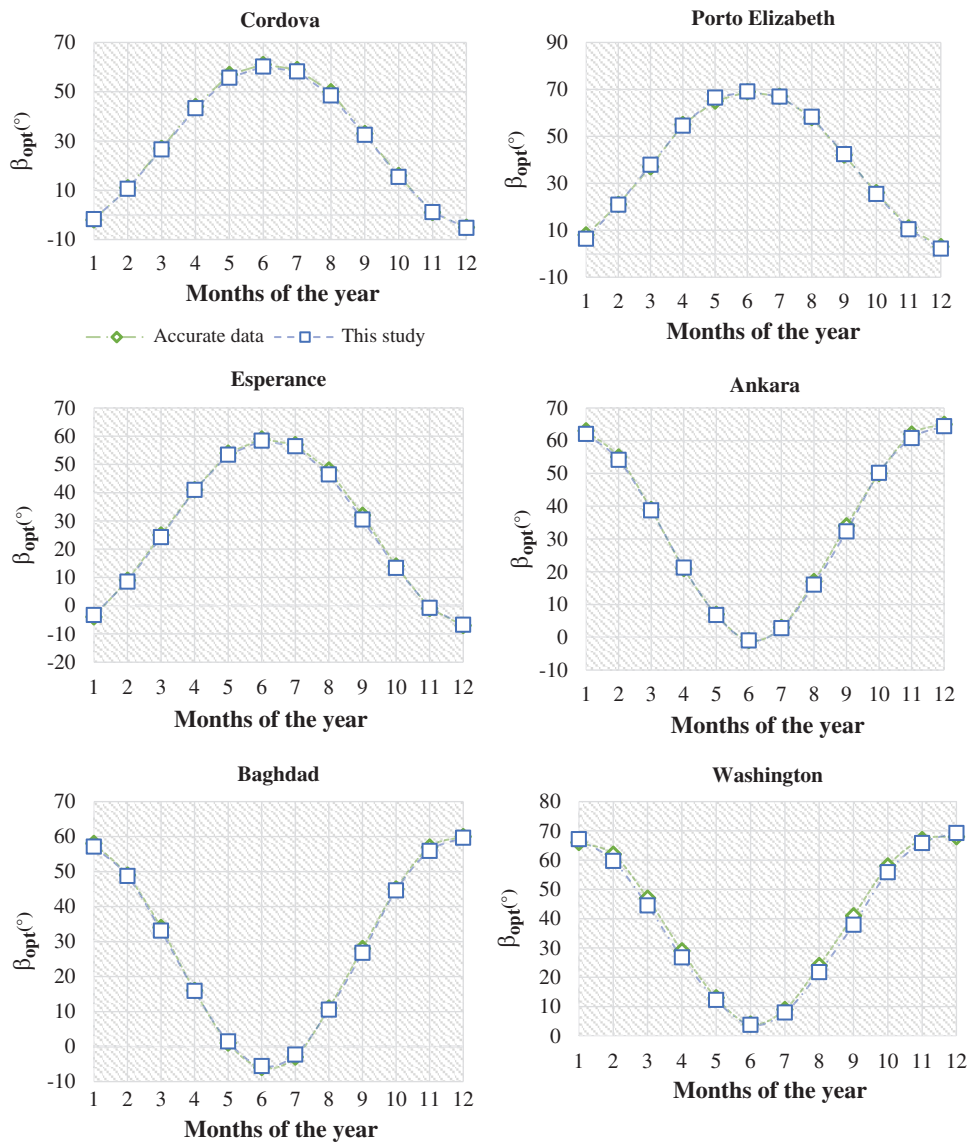
Figure 8: Comparison of the optimum slope angle (calculated and proposed) in the six different stations

The results confirm the 20% increase in solar radiation over collectors considering the monthly tilt angle approach. In some stations, there is no possibility of changing the tilt angle on a monthly basis. The offered method in these cases is the use of a yearly slope angle. Fig. 9, demonstrates the fact that the yearly optimum slope angle can also increase the received solar energy on the collectors around 7%. Several equations are proffered for this target (mentioned in the introduction). Fig. 10 compares the efficiency of the equation, $\beta_{opt} = \pm 0.76575 \varnothing + 3.38°$, that is developed in this study for the horizontal collectors (HC) and Qiu et al. [31], $\beta_{opt} = \varnothing \pm 10°$, Lunde [14], $\beta_{opt} = \varnothing \pm 15°$, Duffie et al. [32], $\beta_{opt} = (\varnothing + 15°) \pm 15°$, Heywood [13], $\beta_{opt} = \varnothing - 10°$, El-Kassaby [33], $\beta_{opt} = \varnothing + 3.5°$, Lewis [34], $\beta_{opt} = \varnothing \pm 8°$, and Yellott [35], $\beta_{opt} = \varnothing + 20°$. The graph illustrates the summation of the average monthly solar radiation for Bushehr (Iran) in the northern hemisphere for a different yearly tilt angle. It is clear that the maximum solar radiation is obtained by employing the proposed correlation in this study. Likewise, this comparison was made for Melbourne (Australia), where the results are shown in Fig. 11.
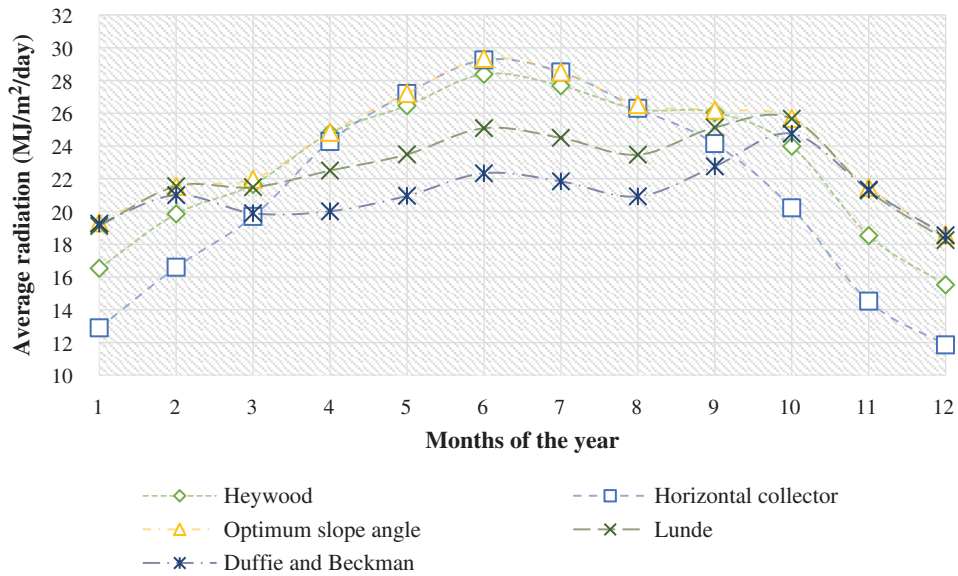
Figure 9: Comparison of the average solar radiation on collectors with different methods
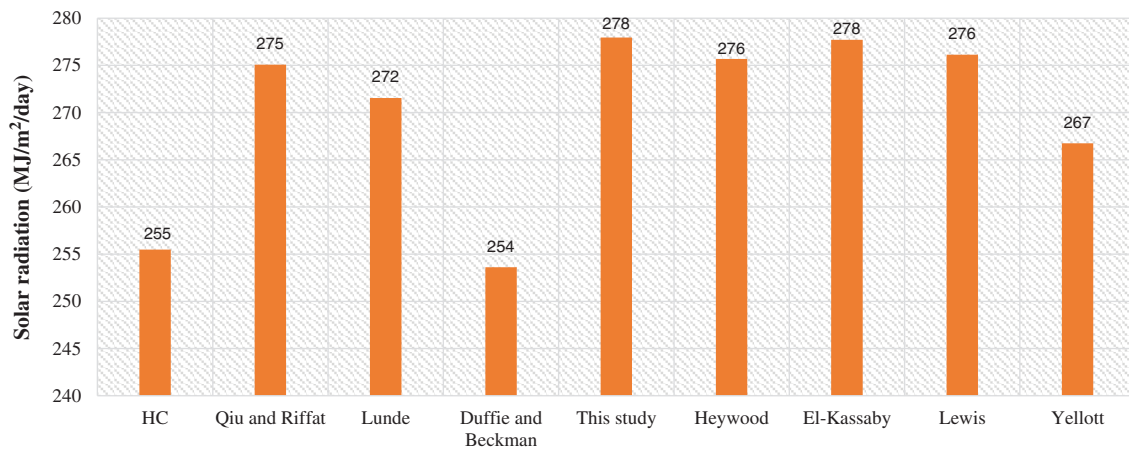
Figure 10: Comparison of the yearly slope angle equations for Bushehr (Iran)
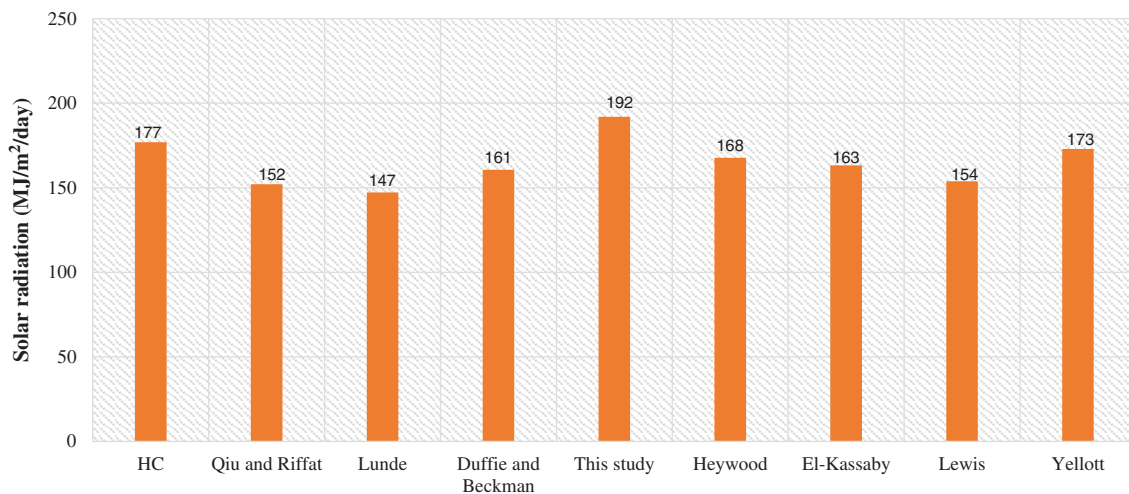
Figure 11: Comparison of the yearly slope angle equations for Melbourne (Australia)

4 Conclusion

Sun tracker systems are new technologies that change the collectors' angle to track the sunray. But these systems are capital intensive, and most often, the maintenance cost is impressive. It is noteworthy that single-axis tracker projects need to consider an additional focus on company stability and bankability because these systems require new technologies that are expensive. Hence determining the optimum slope angle is important for receiving the more solar radiation on flat-plate collectors in case of not using sun trackers. In this study, the optimum slope angle for solar collectors has been analyzed, and the results are explained in the following:

- In this study, 37 stations in the northern hemisphere (latitude: 15 to 55) and 22 stations in the southern hemisphere (latitude: –20 to –45) were analyzed, respectively. For this investigation, the average data from 2000 to 2016 is used. For each month, one equation was proposed to calculate the optimum tilt angle. These correlations are compared with the monthly tilt angle correlations that have been developed by Nijeogorodov et al. [23] and Talebizade et al. [21]. Comparing the proposed models to the literature, results prove a higher accuracy of the introduced equations in this study.
- For the northern and southern hemispheres, one correlation for a yearly tilt angle was developed. This equation was compared with the seven other correlations which were developed by Qiu et al. [31], Lunde [14], Duffie et al. [32], Heywood [13], El-Kassaby [33], Lewis [34], and Yellott [35]. The results demonstrated that the maximum solar radiation was obtained with the proposed yearly angle of this study.
- Analysis of the received solar radiation on the collectors is illustrated by adjusting the collectors with the monthly optimum slope angle leads to an approximately 20% increase in monthly average radiation received from the sun. This increase is higher for January and December (about 50%) than the other months of the year. Also, a 7% increment in solar radiation is observed using a yearly tilt angle method as compared to the fixed horizontal collectors.
- Azimuth angle (for one city in the northern hemisphere (Bushehr, Iran) and southern (Melbourne, Australia) hemisphere) was calculated. The optimum monthly azimuth angle for Bushehr and Melbourne were obtained as 0° and 180°, respectively. This conclusion confirms the hypothesis of the Liu et al. method [27].

Conflicts of Interest: The authors declare that they have no conflicts of interest to report regarding the present study.

References

1. IPCC (2018). Summary for Policymakers. In: Masson-Delmotte, V., Zhai, P., Pörtner, H. O., Roberts, D., Skea, J. et al. (eds.), *Global warming of 1.5°C. An IPCC special report on the impacts of global warming of 1.5°C above pre-industrial levels and related global greenhouse gas emission pathways, in the context of strengthening the global response to the threat of climate change, sustainable development, and efforts to eradicate poverty*, pp. 32. World Meteorological Organization, Geneva, Switzerland. https://www.ipcc.ch/sr15/.
2. Veludurthi, A., Bolleddu, V. (2020). Experimental study on modal and harmonic analysis of small wind turbine blades using NACA 63-415 aerofoil cross-section. *Energy Engineering: Journal of the Association of Energy Engineers, 117(2),* 49–61.
3. Khosravi, A., Syri, S., El Haj Assad, M., Malekan, M. (2019). Thermodynamic and economic analysis of a hybrid ocean thermal energy conversion/photovoltaic system with hydrogen-based energy storage system. *Energy, 172,* 304–319. DOI 10.1016/j.energy.2019.01.100.

4. Khosravi, A., Syri, S., Pabon, J., Sandoval, O., Castro Caetano, B. et al. (2019). Energy modeling of a solar dish/ stirling by artificial intelligence approach. *Energy Conversion and Management, 199,* 112021. DOI 10.1016/j. enconman.2019.112021.

5. Khosravi, A., Olkkonen, V., Farsaei, A., Syri, S. (2020). Replacing hard coal with wind and nuclear power in Finland—impacts on electricity and district heating markets. *Energy, 203,* 117884. DOI 10.1016/j. energy.2020.117884.

6. Malekan, M., Khosravi, A., Syri, S. (2019). Heat transfer modeling of a parabolic trough solar collector with working fluid of Fe_3O_4 and CuO/Therminol 66 nanofluids under magnetic field. *Thermal Engineering, 163,* 114435. DOI 10.1016/j.applthermaleng.2019.114435.

7. Sedaghat, A., Hani, E. H. B., Ali, S., Ali, F., Al-Mesbah, A. et al. (2018). Experimental and theoretical analysis of a solar desalination system improved by thermoelectric cooler and applying sun tracking system. *Energy Engineering: Journal of the Association of Energy Engineers, 115(6),* 62–76.

8. Ehab, B. H., Borgford, C., Khanafer, K. (2016). Applications of porous materials and nanoparticles in improving solar desalination systems. *Journal of Porous Media, 19(11),* 993–999. DOI 10.1615/JPorMedia.v19.i11.50.

9. Khosravi, A., Koury, R. N. N., Machado, L., Pabon, J. J. G. (2018). Prediction of hourly solar radiation in Abu Musa Island using machine learning algorithms. *Journal of Cleaner Production, 176,* 63–75. DOI 10.1016/j. jclepro.2017.12.065.

10. Oğulata, R. T., Oğulata, S. N. (2002). Solar energy potential in Turkey. *Energy Sources, 24(12),* 1055–1064. DOI 10.1080/00908310290086987.

11. Kocar, G., Eryasar, A. (2007). An application of solar energy storage in the gas: solar heated biogas plants. *Energy Sources, Part A: Recovery, Utilization, and Environmental Effects, 29(16),* 1513–1520. DOI 10.1080/ 00908310600626598.

12. Hepbasli, A., Alsuhaibani, Z. (2014). Estimating and comparing the exergetic solar radiation values of various climate regions for solar energy utilization. *Energy Sources, Part A: Recovery, Utilization, and Environmental Effects, 36(7),* 764–773. DOI 10.1080/15567036.2010.545807.

13. Heywood, H. (1971). Operating experiences with solar water heating. *Journal Institution of Heating and Ventilating Engineers, 39,* 63–69.

14. Lunde, P. J. (1980). *Solar thermal engineering: space heating and hot water systems.* New York: John Wiley Sons.

15. Duffie, J., Beckman, W. (2006). *Solar engineering of thermal processes,* 3th ed. pp. 116. Hoboken, New Jersey: John Wiley & Sons, Inc.

16. Bakirci, K. (2012). General models for optimum tilt angles of solar panels: Turkey case study. *Renewable and Sustainable Energy Reviews, 16(8),* 6149–6159. DOI 10.1016/j.rser.2012.07.009.

17. Benghanem, M. (2011). Optimization of tilt angle for solar panel: case study for Madinah, Saudi Arabia. *Applied Energy, 88(4),* 1427–1433. DOI 10.1016/j.apenergy.2010.10.001.

18. Lave, M., Kleissl, J. (2011). Optimum fixed orientations and benefits of tracking for capturing solar radiation in the continental United States. *Renewable Energy, 36(3),* 1145–1152. DOI 10.1016/j.renene.2010.07.032.

19. Ahmad, M. J., Tiwari, G. N. (2009). Optimization of tilt angle for solar collector to receive maximum radiation. *Open Renewable Energy Journal, 2(1),* 19–24. DOI 10.2174/1876387100902010019.

20. Stanciu, C., Stanciu, D. (2014). Optimum tilt angle for flat plate collectors all over the world—a declination dependence formula and comparisons of three solar radiation models. *Energy Conversion and Management, 81,* 133–143. DOI 10.1016/j.enconman.2014.02.016.

21. Talebizadeh, P., Mehrabian, M. A., Abdolzadeh, M. (2011). Determination of optimum slope angles of solar collectors based on new correlations. *Energy Sources, Part A: Recovery, Utilization, and Environmental Effects, 33(17),* 1567–1580. DOI 10.1080/15567036.2010.551253.

22. Talebizadeh, P., Mehrabian, M. A., Abdolzadeh, M. (2011). Prediction of the optimum slope and surface azimuth angles using the genetic algorithm. *Energy and Buildings, 43(11),* 2998–3005. DOI 10.1016/j. enbuild.2011.07.013.

23. Nijegorodov, N., Devan, K. R. S., Jain, P. K., Carlsson, S. (1994). Atmospheric transmittance models and an analytical method to predict the optimum slope of an absorber plate, variously oriented at any latitude. *Renewable and Energy, 4(5),* 529–543. DOI 10.1016/0960-1481(94)90215-1.

24. Elminir, H. K., Ghitas, A. E., El-Hussainy, F., Hamid, R., Beheary, M. M. et al. (2006). Optimum solar flat-plate collector slope: case study for Helwan, Egypt. *Energy Conversion and Management, 47(5),* 624–637. DOI 10.1016/j.enconman.2005.05.015.

25. Kacira, M., Simsek, M., Babur, Y., Demirkol, S. (2004). Determining optimum tilt angles and orientations of photovoltaic panels in Sanliurfa, Turkey. *Renewable Energy, 29(8),* 1265–1275. DOI 10.1016/j. renene.2003.12.014.

26. Ulgen, K. (2006). Optimum tilt angle for solar collectors. *Energy Sources, Part A: Recovery, Utilization, and Environmental Effects, 28(13),* 1171–1180.

27. Liu, B., Jordan, R. (1961). Daily insolation on surfaces tilted towards equator. *Journal of American Society of Heating, Refrigerating and Air-Conditioning Engineers, 3(10),* 53–59.

28. Klein, S. A., Theilacker, J. C. (1981). An algorithm for calculating monthly-average radiation on inclined surfaces. *Journal of Solar Energy Engineering, 103(11),* 29–33. DOI 10.1115/1.3266201.

29. Klein, S. A. (1977). Calculation of monthly average insolation on tilted surfaces. *Solar Energy, 19(4),* 325–329. DOI 10.1016/0038-092X(77)90001-9.

30. Duffie, B., Beckman, W. A. (1982). *Solar engineering of thermal processes*. Hoboken: John Wiley Sons.

31. Qiu, G., Riffat, S. B. (2003). Optimum tilt angle of solar collectors and its impact on performance. *International Journal of Ambient Energy, 24(1),* 13–20. DOI 10.1080/01430750.2003.9674898.

32. Duffie, J., Beckman, W. (2013). *Solar engineering of thermal processes,* 4th ed. pp. 116. Hoboken, New Jersey: John Wiley & Sons, Inc.

33. El-Kassaby, M. M. (1988). Monthly and daily optimum tilt angle for south facing solar collectors: theoretical model, experimental and empirical correlations. *Solar & Wind Technology, 5(6),* 589–596. DOI 10.1016/0741-983X(88)90054-9.

34. Lewis, G. (1987). Optimum tilt of a solar collector. *Solar & Wind Technology, 4(3),* 407–410. DOI 10.1016/0741-983X(87)90073-7.

35. Yellott, J. (1973). Utilization of sun and sky radiation for heating and cooling of buildings. *Journal of American Society of Heating, Refrigerating and Air-Conditioning Engineers, 15(12),* 31–42.